Nat. Hazards Earth Syst. Sci. Discuss., 1, 5545–5560, 2013
www.nat-hazards-earth-syst-sci-discuss.net/1/5545/2013/
doi:10.5194/nhessd-1-5545-2013

Natural Hazards and Earth System Sciences
Discussions
Open Access

Electrical resistivity tomography for studying liquefaction induced by the May 2012 Emilia-Romagna earthquake (M_w = 6.1, North Italy)

A. Giocoli[1,2], B. Quadrio[3], J. Bellanova[1], V. Lapenna[1], and S. Piscitelli[1]

[1]CNR-IMAA, Tito, Potenza, Italy
[2]ENEA, Rome, Italy
[3]CNR-IGAG, Rome, Italy

Received: 16 July 2013 – Accepted: 15 September 2013 – Published: 16 October 2013

Correspondence to: A. Giocoli (alessandro.giocoli@enea.it)

Published by Copernicus Publications on behalf of the European Geosciences Union.

Abstract

This work shows the result of an Electrical Resistivity Tomography survey carried out for imaging and characterizing the shallow subsurface affected by the coseismic effects of the $M_w = 6.1$ Emilia-Romagna (North Italy) earthquake occurred on 20 May 2012. The most characteristic coseismic effects were ground failure, lateral spreading and liquefaction that occurred extensively along the paleo-Reno river in the urban areas of San Carlo, a hamlet of Sant'Agostino municipality, and of Mirabello (south-western portion of the Ferrara Province). Totally, six Electrical Resistivity Tomography were performed and calibrated with surface geological surveys, exploratory borehole and aerial photo interpretations. This was one of the first applications of the Electrical Resistivity Tomography method in investigating coseismic liquefaction.

1 Introduction

On 20 May 2012 a reverse-fault earthquake ($M_w = 6.1$; QRCMT, 2012) hit Emilia-Romagna region (Northern Italy). The hypocenter of the event was 6.3 km depth and the epicenter was localized at 44.889° N and 11.228° E, near the town of Finale Emilia (Fig. 1a). The coseismic effects associated with this event were observed in the nearby villages located within 20–30 km from the epicenter. The most important coseismic effect was related to the occurrence of liquefaction and subsequent formation of ground failures. The most impressive cases were those observed along the paleo-Reno river in the villages of Mirabello and Sant'Agostino (San Carlo hamlet). Here, liquefaction and hundred meters long fractures affected agricultural field, buildings, walls, pipelines and roads, causing severe damage (Fig. 1d) (Galli et al., 2012). In the urban areas of Mirabello and San Carlo, we investigated, by mean of an Electrical Resistivity Tomography (ERT) survey, the subsurface surrounding some of the major superficial manifestations of liquefaction. In all cases, we used surface geological surveys, exploratory boreholes and aerial photo interpretations to calibrate the electrical resistivity models and to directly correlate resistivity values with the lithostratigraphic characteristics. The main aim of the ERT investigation was to provide rapid and valuable geological information (e.g. shape, thickness and depth of the different geological units, depth of the water table, etc.) on the uppermost part of the subsoil affected by the coseismic liquefaction.

2 Geological and geomorphological framework

The epicentral area of the 20 May 2012 Emilia-Romagna earthquake is located south of the Po River, in correspondence of the active front of the northern Apennines trust belt that is composed of buried folds and trust faults verging to the north (Fig. 1a). This area is a morphologically uniform sector of the Po Plain with modest reliefs in correspondence with the natural levees of the water courses, the banks of the abandoned river channels and the anthropogenic backfills. Most of the liquefaction effects occurred between San Carlo and Mirabello along the paleo-Reno river (15th–18th century). Here, the witnesses of the past hydrography are still marked in the local topography. In particular, the bed (about 12 m a.s.l.), the lateral banks (about 16.5 m a.s.l.) and the floodplain (about 13 m a.s.l.) of the paleo-Reno river are still well preserved. Recent very detailed investigation at San Carlo and Mirabello (Calabrese et al., 2012) allowed us to reconstruct the shallow sub-surface stratigraphy within the first 15–20 m (usual depth range for liquefaction occurrence, Youd et al., 2001). Essentially, three main units were identified.

The upper unit, referred to as Fluvial Channel Unit (FCU), consists prevalently of channel, anthropogenic backfill, riverbank and flood deposits. The FCU is distinguished in three sub-units: (1) paleo-riverbank (raised area at the side of the paleo-riverbed) made up of fine sand alternating with sandy silt in the most proximal portion, passing laterally (distal riverbanks) to sandy silts and clay; (2) paleo-riverbed (topographic low between the paleo-riverbanks) composed of gravel and sand with lenticular shape; (3) anthropogenic backfill and reworked deposits. The FCU is extended to an average depth of 15 m from ground level variable between 8 and 20 m, depending on the considered point. At the bottom, the FCU consists of lenses of medium to fine gray sands (MFGS), which reach their maximum thickness (about 6 m) in the borehole S10 (grey horizon in borehole logs, Fig. 2). These lenses of medium to fine gray sands are proved to have been responsible for the coseismic surface effects (Calabrese et al., 2012).

The intermediate unit, referred to as Marshes Unit (MU), consists mainly of clay and silt with abundant organic portion and levels of peat at different stratigraphic depths. This unit testifies the presence of extensive and persistent marshy areas ("valleys"), in which Apenninic rivers flow into, which have developed from the maximum Holocene transgression. These environments, not disturbed by fluvial and anthropogenic activities, remained until modern times. The estimated average thickness of MU is between 5–10 m and 10–15 m depending on the area.

The lowest stratigraphical unit is the Pleistocene Alluvial Plain Unit (PAPU) that consists of an alternation of sandy silts and silty sands to the roof of an extended and continuous horizon of medium and fine sands. The depth of PAPU is about 25 m below the paleo-riverbanks and 15–20 m in the plain.

3 Electrical Resistivity Tomography

The Electrical Resistivity Tomography (ERT) is an active geophysical method applied to obtain high-resolution images of the subsurface resistivity pattern. In the last years, the ERT is being increasingly applied for studying the active faults (Galli et al., 2006; Improta et al., 2010; Giocoli et al., 2011), the volcanic areas (Finizzola et al., 2010; Siniscalchi et al., 2010), the landslides (Perrone et al., 2004), the geological and structural setting of the basins (Giocoli et al., 2008), the local seismic response (Boncio et al., 2011; Mucciarelli et al., 2011; Moscatelli et al., 2012), etc. Only in very few cases the ERT was applied in laboratory experiments in order to study liquefaction phenomenon during and after the shaking (Jinguuji et al., 2007).

In this paper we present one of the first applications of the ERT method in investigating coseismic liquefaction. Several ERT were carried out in order to image and characterize the shallow subsurface of the areas affected by the coseismic effects of the Emilia-Romagna (North Italy) earthquake occurred on 20 May 2012. In particular, we carried out two ERT in Mirabello and four ERT in San Carlo along the paleo-Reno river, where the ground failure and liquefaction occurred extensively.

All the ERT were performed by means of a Syscal R2 (Iris Instruments) resistivity meter, coupled with a multielectrode acquisition system (48 electrodes). A constant spacing "a" (5 m) between adjacent electrodes was used. Due to limited number of electrodes of the system, in some case we used the roll-along method to extend horizontally the ERT profile. The length of each ERT profile ranged from 235 to 355 m (roll-along profiles). Along each profile, we applied different array configurations (Wenner, Wenner–Schlumberger and Dipole–Dipole) and different combinations of dipole length (1a, 2a and 3a) and "*n*" number of depth levels ($n \leq 6$), obtaining investigation depths of about 35–40 m. The Wenner, Wenner–Schlumberger and Dipole–Dipole apparent resistivity data were inverted using the RES2DINV software (Loke, 2001) to obtain the 2-D resistivity models of the subsurface. For each ERT we present the 2-D resistivity model obtained from array configuration that allowed to acquire data with the higher signal-to-noise (s/n) ratio, a larger investigation depth and a better sensitivity pattern to both horizontal and vertical changes in the subsurface resistivity. The Wenner–Schumberger array given the best result. In all cases, the Root Mean Squared (RMS) error is less than 7.0 % and the resistivity values range from 5 to more than 127 Ωm.

Generally, since the electrical resistivity of a rock is controlled by different factors (water content, porosity, clay content, etc.), there are wide ranges in resistivity for any particular rock type and, accordingly, resistivity values cannot be directly interpreted in terms of lithology. In addition, the interpretation of resistivity data can be ambiguous due to well-known principles of equivalence and suppression (Kunetz, 1966). For these reasons, we used data gathered through geological surveys and exploratory boreholes

Title Page
Abstract Introduction
Conclusions References
Tables Figures
◀| |▶
◀ ▶
Back Close
Full Screen / Esc
Printer-friendly Version
Interactive Discussion

to calibrate the ERT and to directly correlate resistivity values with the lithostratigraphic characteristics. In general, the higher resistivity values ($\rho > 15\,\Omega\text{m}$) are associated to the Fluvial Channel Unit (FCU), the medium resistivity values ($13 < \rho < 40\,\Omega\text{m}$) are attributed to the Pleistocene Alluvial Plain Unit (PAPU) and the lower resistivity values ($\rho < 20\,\Omega\text{m}$) are related to the Marshes Unit (MU).

3.1 San Carlo

The ERT1 and ERT2 were carried out in the northeast sector of San Carlo, a hamlet of Sant'Agostino municipality (Fig. 1b). The first one was performed across the paleo-bed of the Reno river, whereas the second one was carried out along the paleo-bank of the Reno river. The two profiles crossing each other by 90°. At the intersection, both electrical resistivity models (ERT1 and ERT2) show the same resistivity distribution (Fig. 3). This is an evidence of the good quality of data, as the ERT1 and ERT2 were acquired and processed independently.

The ERT3 and ERT4 were carried out across the paleo-bed of the Reno river, in the west part of San Carlo and near the cemetery, respectively (Fig. 1b). In particular, the south part of the ERT3 profile crossed between 125 and 295 m a "Red Zone", where extensive liquefaction and fractures affected buildings, pipelines and roads, causing severe damage.

Generally, all electrical resistivity models put in evidence three plane-parallel layers with different thickness and resistivity values. In agreement with borehole data (Fig. 2) and geological observation (Fig. 1b), the surface layer (thickness < 20 m) of higher resistivity values ($\rho > 15\,\Omega\text{m}$) can be attributed to the alternation of sand and silt of the FCU, the intermediate layer (average thickness about 15 m) of lower resistivity values ($\rho < 20\,\Omega\text{m}$) can be associated prevalently to the silty clay of the MU and the lower layer of medium resistivity values ($13 < \rho < 40\,\Omega\text{m}$) can be related to the sandy silt of the PAPU.

Based on the comparison between the exploratory borehole data and the ERT, we noted an overlap of the resistivity ranges. In particular, the resistivity values included between 15 and 20 are common to the FCU and MU, whereas the resistivity values between 13 and 20 can be associated to both MU and PAPU. This could be due to the rather similar lithologies near the stratigraphic boundary between FCU and MU and between MU and PAPU. Furthermore, the bottom of the FCU could also show similar low-resistivity values to those of the MU due to the presence of the saturated, medium to fine sand (MFGS). Thus, since we could not precisely locate the FCU-MU and MU-PAPU boundaries, we were forced to represent with a diagonal and dotted patterns (T1 and T2) the uncertainity of theirs locations.

3.2 Mirabello

The ERT5 runs NW-SE across the paleo-bed of the Reno river. It crossed between 90 and 235 m a soccer field and a car parking. The ERT6 was carried out prevalently on MU. It can be considered the southeastward continuation of the ERT5 (see Fig. 1c). The ERT5 and ERT6 profiles were not combined in a single long profile, by applying a roll-along acquisition method, due to logistical conditions (presence of a main road). In this case, there are no borehole data that could aid in constraining the interpretation of electrical models. However, it was possible to interpret both resistivity models on the basis of the data coming from superficial geological observation.

Considering both resistivity models, from 65 to 300 m between about 5 and 17 m a.s.l., it is possible to observe a high resistivity sector ($\rho > 15\,\Omega$m) that could be associated to the alternation of sand and silt of the FCU. Below 5 m a.s.l. down to about 0 m a.s.l., both models show a low-resistivity layer ($\rho < 20\,\Omega$m) that could be associated to the silty clay of the MU observed on surface along the ERT6 profile. At the bottom of both resistivity models (below about 0 m a.s.l.), a medium resistivity sector ($13 < \rho < 40\,\Omega$m) could be related to the sandy silt of the PAPU. Also in this case, we used the two transition zone (T1 and T2) to represent the uncertainty of the FCU-MU and MU-PAPU boundaries. We cannot exclude the possibility that the resistivity transition zone (T1), in particular below the high resistivity layer in the ERT5, could be also related to the MFGS at the bottom of the FCU (Fig. 5).

4 Conclusions

A few days after the main shock of the 20 May 2012 Emilia-Romagna (North Italy) earthquake ($M_w = 6.1$), we performed an Electrical Resistivity Tomography survey to investigate the subsurface surrounding some of the major superficial manifestations of coseismic liquefaction in the urban areas of San Carlo and Mirabello. The ERT were used as a reconnaissance method to detect the litostratigraphic characteristics in areas with limited or nonexistent subsoil data.

In particular, this paper documents one of the first applications of ERT method in investigating of coseismic liquefaction.

In all cases, we used surface geological surveys, exploratory boreholes and aerial photo interpretations to calibrate the electrical resistivity models and to directly correlate resistivity values with the lithostratigraphic characteristics. We have also taken into account the results obtained by Abu Zeid et al. (2012), who also investigated coseismic liquefaction only in San Carlo a few weeks after the main seismic event of 20 May 2012. By comparing and matching all these data, we succeed in imaging the lithostratigraphic setting across the superficial manifestations of coseismic liquefaction. In particular, our investigations put in evidence:

- a surficial layer with higher resistivity values ($\rho > 15$) related to FCU (thickness < 20 m);
- an intermediate layer with lower resistivity values ($\rho < 20\,\Omega$m) related to MU (average thickness 10–15 m);
- a lower layer with low-medium resistivity values ($13 < \rho < 40\,\Omega$m) related to PAPU.

The ERT do not clearly reveal the potentially liquefiable level (MFGS) at the bottom of the FCU because the resistivity values of this thin layer (thickness < 6.5 m in the boreholes, see Fig. 2) are similar to those of the MU. Thus, the resistivity transition zone (T1) can be related to the MU or to the bottom of the FCU (i.e. MFGS).

On the bases of ERT results, it was possible to design further investigations (e.g. complementary geophysical surveys, drill holes, etc.) for a better understanding of the liquefaction phenomenon. In conclusion, taking into account all the above inferences, the ERT has proved to be an effective reconnaissance technique for characterizing the subsoil affected by coseismic liquefaction, providing valuable data for understanding the liquefaction phenomenon and assessing the associated hazard.

Acknowledgements. This work was funded by the Department of Civil Protection, Rome. We also thank all the Working Group involved in the study of liquefaction phenomena induced by the May 2012 Emilia Romagna earthquake for the discussions during the advancement of the work.

References

Abu Zeid, N., Bignardi, S., Caputo, R., Santarato, G., and Stefani, M.: Electrical resistivity tomography investigation of coseismic liquefaction and fracturing at San Carlo, Ferrara Province, Italy, Ann. Geophys.-Italy, 55, 713–716, doi:10.4401/ag-6149, 2012.

Boncio, P., Pizzi, A., Cavuoto, G., Mancini, M., Piacentini, T., Miccadei, E., Cavinato, G. P., Piscitelli, S., Giocoli, A., Ferretti, G., De Ferrari, R., Gallipoli, R., Mucciarelli, M., Di Fiore, V., Naso, G., Giaccio, B., Moscatelli, M., Spadoni, M., Romano, G., Franceschini, A., Spallarossa, D., Pasta, M., Pavan, M., Scafidi, D., Barani, S., Eva, C., Pergalani, F., Compagnoni, M., Campea, T., Di Berardino, G. R., Mancini, T., Marino, A., Montefalcone, R., and Mosca, F.: Geological and geophysical characterization of the Paganica – San Gregorio area after the April 6, 2009 L'Aquila earthquake (Mw 6.3, central Italy): implications for site response, B. Geofis. Teor. Appl., 52, 491–512, doi:10.4430/bgta0014, 2011.

Calabrese, L., Martelli, L., and Severi, P.: Stratigrafia dell'area interessata dai fenomeni di liquefazione durante il terremoto dell'Emilia (maggio 2012), 31th GNGTS, Trieste, Italy, 20–22 November 2012, 119–126, available at: http://www2.ogs.trieste.it/gngts/, last access: October 2013, 2012.

CNR-PFG (Progetto Finalizzato Geodinamica): Synthetic structural-kinematic map of Italy, in: Structural Model of Italy and Gravity Map, Quaderni de la Ricerca Scientifica, S.EL.CA., Firenze, Sheet n. 5, 1991.

Finizola, A., Ricci, T., Deiana, R., Barde Cabusson, S., Rossi, M., Fraticelli, N., Giocoli, A., Romano, G., Delcher, E., Suski, B., Revil, A., Menny, P., Di Gangi, F., Letort, J., Peltier, A., Villasante-Marcos, V., Douillet, G., Avard, G., and Lelli, M.: Adventive hydrothermal circulation on Stromboli volcano (Aeolian Islands, Italy) revealed by geophysical and geochemical approaches: implications for general fluid flow models on volcanoes, J. Volcanol. Geoth. Res., 196, 111–119, doi:10.1016/j.jvolgeores.2010.07.022, 2010.

Galli, P., Bosi, V., Piscitelli, S., Giocoli, A., and Scionti, V.: Late Holocene earthquakes in southern Apennines: paleoseismology of the Caggiano fault, Int. J. Earth Sci., 95, 855–870, doi:10.1007/s00531-005-0066-2, 2006.

Galli, P., Castenetto, S., and Peronace, E.: The MCS macroseismic survey of the Emilia 2012 earthquakes, Ann. Geophys.-Italy, 55, 663–672, doi:10.4401/ag-6163, 2012.

Giocoli, A., Magrì, C., Piscitelli, S., Rizzo, E., Siniscalchi, A., Burrato, P., Vannoli, P., Basso, C., and Di Nocera, S.: Electrical Resistivity Tomography Investigations in the Ufita Valley (Southern Italy), Ann. Geophys.-Italy, 51, 213–223, 2008.

Giocoli, A., Galli, P., Giaccio, B., Lapenna, V., Messina, P., Peronace, E., Piscitelli, S., and Romano, G.: Electrical Resistivity Tomography across the Paganica-San Demetrio fault system (April 2009 L'Aquila earthquake, Mw 6.3), B. Geofis. Teor. Appl., 52, 457–469, doi:10.4430/bgta0029, 2011.

Improta, L., Ferranti, L., De Martini, P. M., Piscitelli, S., Bruno, P. P., Burrato, P., Civico, R., Giocoli, A., Iorio, M., D'addezio, G., and Maschio, L.: Detecting young, slow-slipping active faults by geologic and multidisciplinary high-resolution geophysical investigations: a case study from the Apennine seismic belt, Italy, J. Geophys. Res., 115, B11307, doi:10.1029/2010JB000871, 2010.

Jinguuji, M., Toprak, S., and Kunimatsu, S.: Visualization technique for liquefaction process in chamber experiments by using electrical resistivity monitoring, Soil Dyn. Earthq. Eng., 27, 191–199, doi:10.1016/j.soildyn.2006.08.004, 2007.

Kunetz, G.: Principles of Direct Current Resistivity Prospecting, Gebruder Borntraeger, Berlin-Nikolassee, 103 pp., 1966.

Loke, M. H.: Tutorial: 2-D and 3-D electrical imaging surveys, available at: http://www.geoelectrical.com, last access: June 2013, 2001.

Moscatelli, M., Pagliaroli, A., Mancini, M., Stigliano, F., Cavuoto, G., Simionato, M., Peronace, E., Quadrio, B., Tommasi, P., Cavinato, G. P., Di Fiore, V., Angelino, A., Lanzo, G., Piro, S., Zamuner, D., Di Luzio, E., Piscitelli, S., Giocoli, A., Perrone, A., Rizzo, E., Romano, G., Naso, G., Castenetto, S., Corazza, A., Marcucci, S., Cecchi, R., and Petrangeli, P.: Integrated subsoil model for seismic microzonation in the Central Archaeological Area of Rome (Italy), Disaster Advances, 5, 109–124, 2012.

Mucciarelli, M., Bianca, M., Ditommaso, R., Vona, M., Gallipoli, M. R., Giocoli, A., Piscitelli, S., Rizzo, E., and Picozzi, M.: Peculiar earthquake damage on a reinforced concrete building in San Gregorio (L'Aquila, Italy): site effects or building defects?, B. Earthq. Eng., 9, 825–840, doi:10.1007/s10518-011-9257-3, 2011.

Perrone, A., Iannuzzi, A., Lapenna, V., Lorenzo, P., Piscitelli, S., Rizzo, E., and Sdao, F.: High-resolution electrical imaging of the Varco d'Izzo earthflow (southern Italy), J. Appl. Geophys., 56, 17–29, 2004.

QRCMT: Quick Regional Centroid Moment Tensor, INGV-Bologna, available at: http://autorcmt.bo.ingv.it/quicks.html, last access: June 2013, 2012.

Siniscalchi, A., Tripaldi, S., Neri, M., Giammanco, S., Piscitelli, S., Balasco, M., Behncke, B., Magrì, C., Naudet, V., and Rizzo, E.: Insights into fluid circulation across the Pernicana Fault (Mt. Etna, Italy) and implications for flank instability, J. Volcanol. Geoth. Res., 193, 137–142, doi:10.1016/j.jvolgeores.2010.03.013, 2010.

Youd, T. L., Idriss, I. M., Andrus, R. D., Arango, I., Castro, G., Christian, J. T., Dobry, R., Liam Finn, W. D., Harder, L. F., Hynes, M. E., Ishihara, K., Koester, J. P., Liao, S. S., Marcuson, W. F., Martin, G. R., Mitchell, J. K., Moriwaki, Y., Power, M. S., Robertson, P. K., Seed, R. B., and Stoke, K. H.: Liquefaction resistance of Soils: summary report from the 1996 NCEER and 1998 NCEER/NSF workshops on evaluation of liquefaction resistance of soils, J. Geotech. Geoenviron., 127, 817–833, 2001.

Title Page
Abstract | Introduction
Conclusions | References
Tables | Figures
◀| |▶
◀ ▶
Back | Close
Full Screen / Esc
Printer-friendly Version
Interactive Discussion

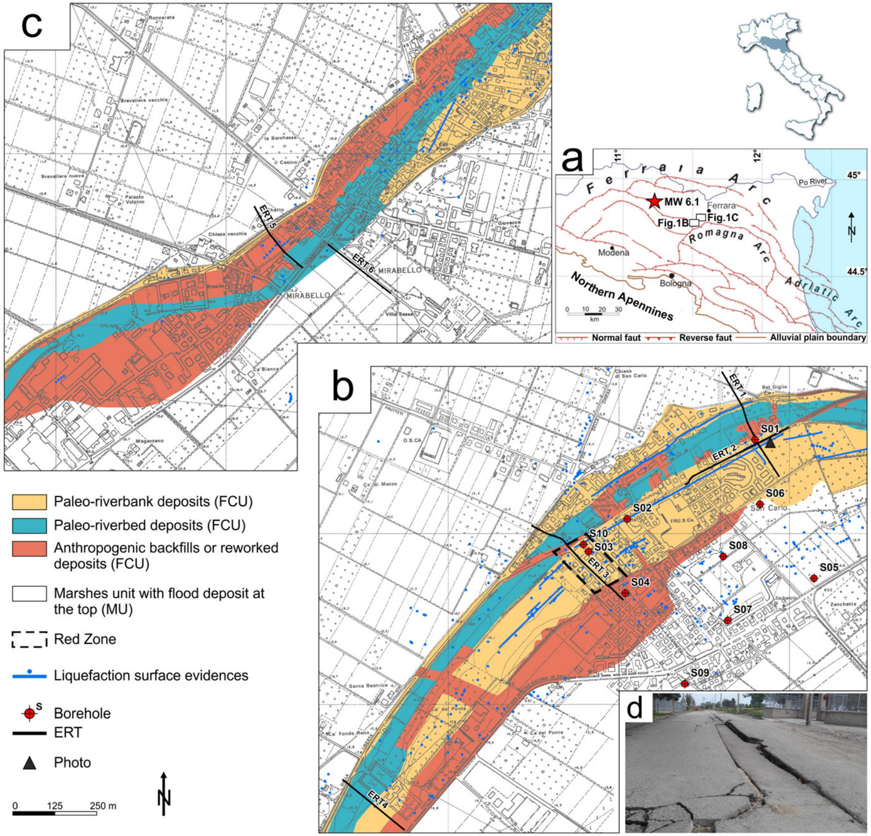

Fig. 1. (A) Simplified tectonic map showing the epicentre of the 20 May 2012 Emilia-Romagna earthquake (modified from CNR-PFG, 1991). Sketch map of the surface deposits derived from digital elevation models, field observations and boreholes. **(B)** San Carlo, hamlet of Sant'Agostino. **(C)** Mirabello. Black triangle is the location of photo **(D)**.

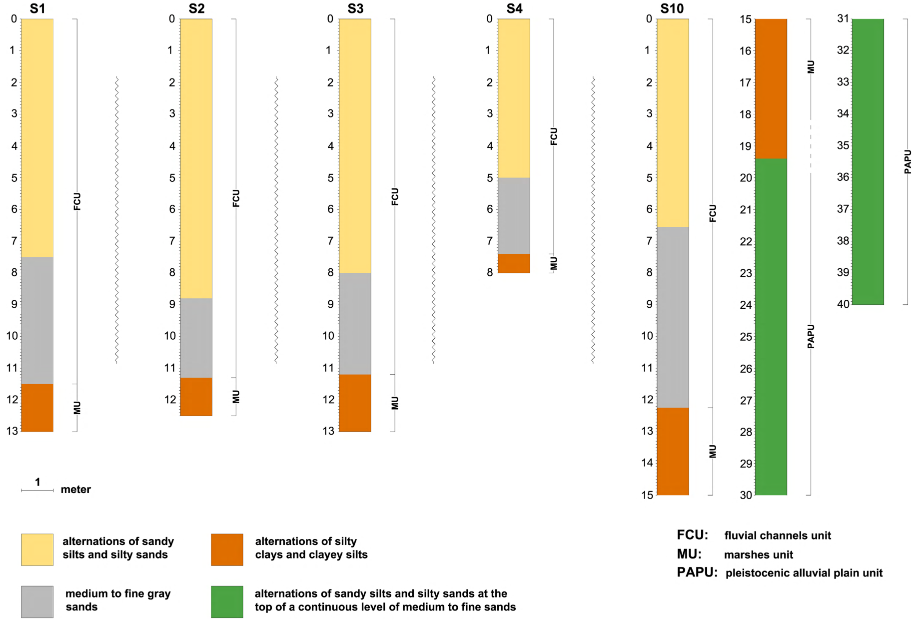

Fig. 2. Five borehole logs used to calibrate the ERT (see Fig. 1 for each borehole location).

Title Page
Abstract
Introduction
Conclusions
References
Tables
Figures
◀▮
▶▮
◀
▶
Back
Close
Full Screen / Esc
Printer-friendly Version
Interactive Discussion

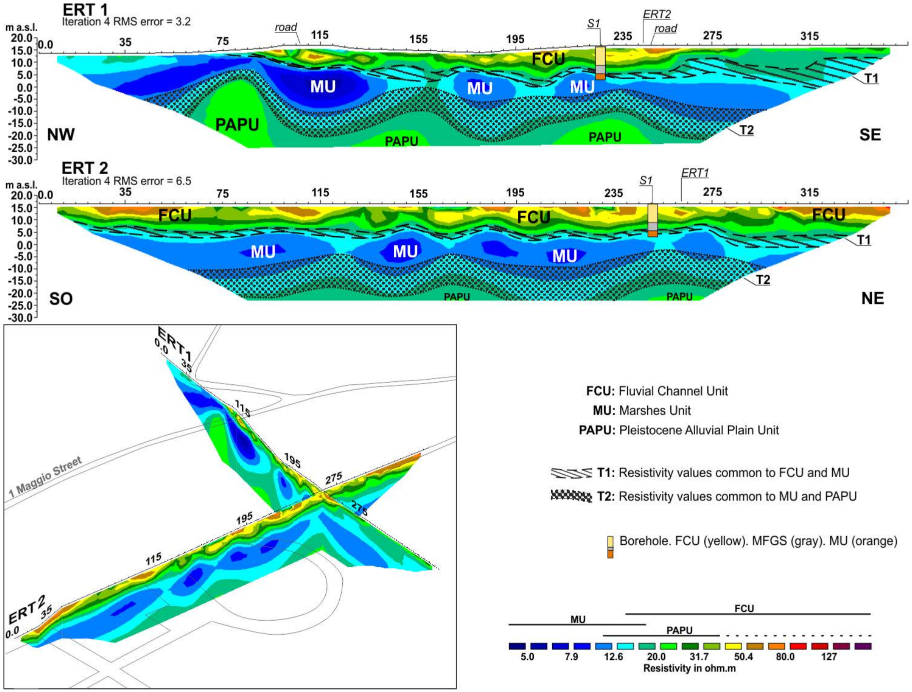

Fig. 3. ERT1 and ERT2 carried out in the northeast sector of San Carlo (see Fig. 2a for location of ERT).

Title Page
Abstract Introduction
Conclusions References
Tables Figures
◀| |▶
◀ ▶
Back Close
Full Screen / Esc
Printer-friendly Version
Interactive Discussion

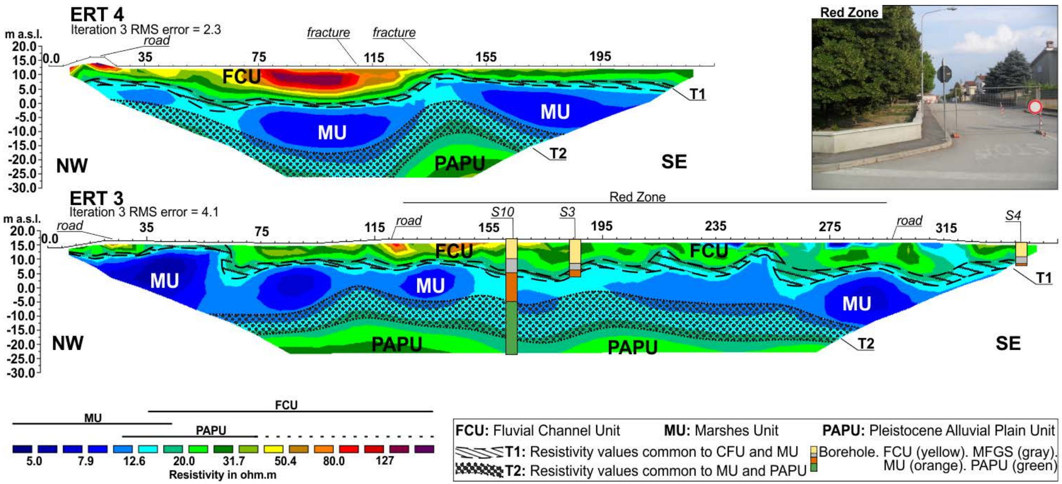

Fig. 4. ERT3 and ERT4 carried out in the west part of San Carlo and near the cemetery, respectively (see Fig. 2a for location of ERT).

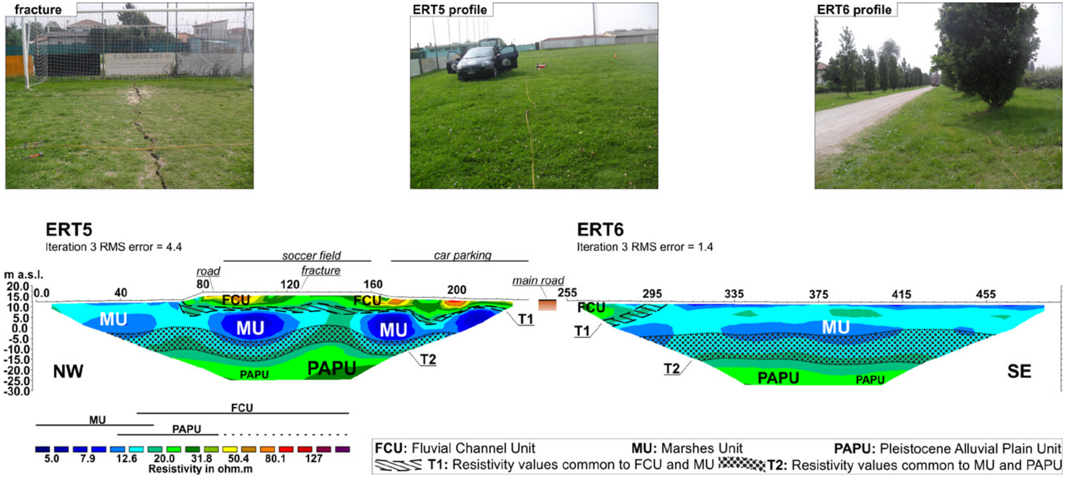

Fig. 5. ERT5 and ERT6 carried out in Mirabello.

Title Page
Abstract
Introduction
Conclusions
References
Tables
Figures
◀|
|▶
◀
▶
Back
Close
Full Screen / Esc
Printer-friendly Version
Interactive Discussion